

## Laminated, microfluidic-integrated carbon nanotube based biosensors

Ju Nie Tey,<sup>1</sup> I Putu Mahendra Wijaya,<sup>1,a)</sup> Zongbin Wang,<sup>1</sup> Wei Hau Goh,<sup>1</sup> Alagappan Palaniappan,<sup>1</sup> Subodh G. Mhaisalkar,<sup>1,b)</sup> Isabel Rodriguez,<sup>2</sup> Simon Dunham,<sup>3</sup> and John A. Rogers<sup>3</sup>

<sup>1</sup>*School of Materials Science and Engineering, Nanyang Technological University, Singapore 639798, Singapore*

<sup>2</sup>*Institute of Materials Research and Engineering, 3 Research Link, Singapore 117602, Singapore*

<sup>3</sup>*Department of Materials Science and Engineering, University of Illinois at Urbana-Champaign, Illinois 61801, USA and Department of Chemistry, University of Illinois at Urbana-Champaign, Illinois 61801, USA*

(Received 6 October 2008; accepted 15 December 2008; published online 8 January 2009)

In this communication, a laminated, flexible, microfluidic-integrated, all CNT based liquid-gated transistor and biosensor are reported that comprises single walled CNTs for both the semiconducting channel as well as the contact electrodes. The proposed architecture eliminates the need for lithography, electrode definition processes, and also circumvents substrate surface compatibility issues. Real-time detection of 1 pM poly-L-lysine in a liquid-gated transistor comprising only two materials, single walled CNTs and polydimethoxysilane substrate with microfluidic channel, is demonstrated. © 2009 American Institute of Physics. [DOI: 10.1063/1.3065480]

Single walled carbon nanotubes (SWCNTs) have sparked considerable interest in biosensing applications due to their exceptional charge transport properties and size compatibility (diameter of  $\sim 1$  nm) with biomolecules.<sup>1</sup> Electrochemical and field effect transistor (FET) based CNT biosensors have been demonstrated. In the former, CNTs are incorporated into the electrode and electrochemical tags are typically required. The “label-free” FET detection methodology utilizes the SWCNTs as “channel modulation labels” to sense changes in their immediate environment as a result of specific interactions with biomolecules. In addition to dry state offline sensing,<sup>2</sup> real-time detection has been demonstrated in a liquid-gated (LG) configuration,<sup>3,4</sup> where the electrolyte replaces the dielectric in normal operation. The electrical double layer capacitance created by the electrolyte and high surface area of the SWCNT network yields a total gate capacitance that is an order of magnitude higher than that of a typical Si/SiO<sub>2</sub> bottom gate configuration.<sup>5</sup> This effectively reduces the gate sweeping potential, allowing a complete on-off swing in less than 1 V. LG-CNTFETs have been typically fabricated on silicon substrates where the SWCNTs are grown by chemical vapor deposition (CVD) and metal electrodes are patterned subsequently. Liquid and analytes are delivered by a microfluidic channel, usually made of polydimethylsiloxane (PDMS) and placed on top of the FET channel. The electrodes need to be passivated to reduce gate leakage, and the biomolecule substrate interactions need to be carefully considered so as to avoid any interference with analyte detection.

This communication reports a facile method of fabricating LG-CNTFETs that consist of simple process steps and do not require the use of lithography or electrode metal deposition processes. Only two materials are required for the fabrication: PDMS (Sylgard 184, Dow Corning, Inc.) and

SWCNT powder (P2-SWCNT, Carbon Solutions, Inc.). Microchannels are first fabricated in PDMS by casting a 10:1 ratio of uncured resin and curing agent in a silicon master mold. The as-purchased SWCNT powder is heated to 900 °C in inert environment for 2 h to eliminate carboxyl groups that may cause electrochemical current leaking from the nanotube network to the reference electrode.<sup>6</sup> A suspension of 0.1 mg/ml CNT in 1% sodium dodecyl sulfate was sonicated, followed by centrifugation for 1 h at 14 000 rpm to remove the nondispersed bundles from the suspension. SWCNT films are prepared by vacuum filtration of the suspension.<sup>7</sup> Tuning the sheet resistance  $R_s$  is facilitated by controlling the filtration volume, hence, the density of the nanotube network films. Films with  $R_s$  larger than 300 k $\Omega$ /sq are used as the transistor channel, whereas, films with  $R_s$  less than 1 k $\Omega$ /sq are employed for fabricating the source and drain contact pads. SWCNTs with 1 k $\Omega$ /sq  $R_s$  are transferred to flat PDMS slabs. SWCNTs with 300 k $\Omega$ /sq  $R_s$  are transferred by stamping to the PDMS substrates carrying the microfluidic channel. Stamping PDMS carrier with the microfluidic channel (400  $\mu$ m) defines automatically the SWCNT source and drain electrodes and also the channel length ( $L$ ) of the transistor (Fig. 1) with only minimal alignment required between the PDMS substrates and the CNT pad area. The lamination process is completed by bringing together the two PDMS carriers. Ensuring the cleanliness of the two carriers is essential for self-sealing of both PDMS surfaces. Devices fabricated with width/length ( $W/L$ ) ratio of 2000/400  $\mu$ m yielded resistances of 20–25 k $\Omega$ .

Electrical measurement of the laminated LG-CNTFET followed similar testing protocols as published in the literature,<sup>8</sup> where a liquid gate potential was applied to the reference electrode with respect to the grounded source electrode and a small drain bias of 10 mV applied over the source and drain electrodes to monitor device conductance. A low leak flexible reference electrode (3M KCl, FLEXREF, World Precision Instruments) was used to create stable gate potential and to avoid sensing artifacts.<sup>9</sup> All measurements

<sup>a)</sup>Also at Institute of Materials Research and Engineering, 3 Research Link, Singapore 117602.

<sup>b)</sup>Author to whom correspondence should be addressed. Electronic mail: subodh@ntu.edu.sg.

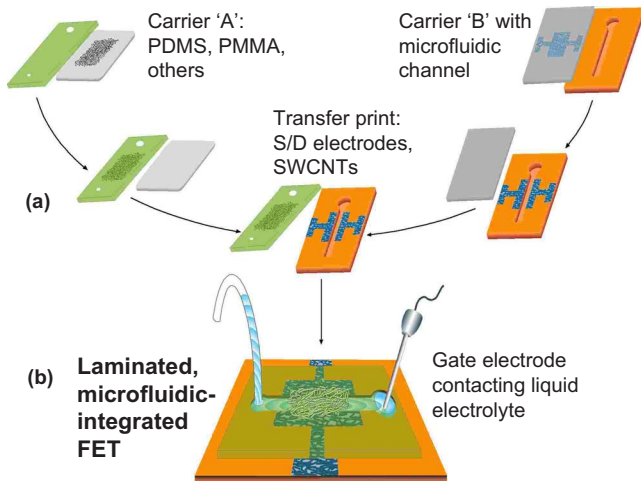


FIG. 1. (Color online) (a) Fabrication process flow for PDMS-laminated LG-CNTFET. A thin SWCNT network obtained by solution processing/filtration is stamped and transferred onto a PDMS substrate (top left, green substrate). A dense SWCNT network with defined source-drain pad and channel width ( $w$ ) is stamped onto another PDMS substrate (top right, orange substrate) with microfluidic channels defined on it by casting. The channel length ( $l$ ) of the transistor is autodefined by the width of the microchannel. The transistor fabrication process is completed by sealing against both PDMS substrates. (b) Top view of the LG-CNTFET.

were conducted in a low ionic strength buffer (LISB) composed of 0.5 mM phosphate buffer and 1.5 mM NaCl ( $pH \sim 7.5$ ). A poly-L-lysine (PLL) solution (p-4707, Sigma Aldrich) was introduced into the fluidic channel using a syringe to examine the real-time sensing capability of the laminated LG-CNTFET.

Typical transfer characteristics ( $I_{sd}-V_g$ ) and time dependent conductance measurements ( $V_g = -60$  mV) for the laminated LG-CNTFET are presented in Figs. 2(a) and 2(b), respectively. Initially the system stability was examined by drawing LISB into the microchannel while recording the signal level. Only small signal disturbances were recorded that may be readily associated with the renewal, and the stabilization of the electrical double layer capacitance as new electrolyte is pumped in. After flushing several times with LISB, a PLL with a concentration of 1 nM was injected into the electrolyte reservoir. Another signal fluctuation was observed, followed by restoration, which implies that the transfer characteristic truly reflects the response at the nanotubes channel-electrolyte interface embedded in the middle of the microchannel. Upon drawing PLL into the microchannel, the  $I_{sd}-V_g$  curve shifted by  $-0.1$  V to the negative direction.

To validate the sensing response of solution prepared-laminated LG-CNTFETs, measurements were carried out using a CVD grown CNT network on Si substrate. As one can observe from Figs. 2(a) and 2(c), differences are noted in the transistor characteristic of the stamped CNT network as opposed to the CVD grown device, with on-off ratios of generally  $< 2$  and high off currents. This may be comprehended based on atomic force microscopy (AFM) images [Figs. 2(a) and 2(c)], which show that the stamped device has much larger bundle sizes and denser CNT networks compared to the CVD grown CNTs. Hence, the likelihood of metallic tube pathways across the electrodes is much higher, leading to high off currents and lower on-off ratios. Nevertheless, these differences in the transfer characteristics do not affect the sensing capability as clearly demonstrated by similar threshold voltage shifts in both the stamped and CVD devices.

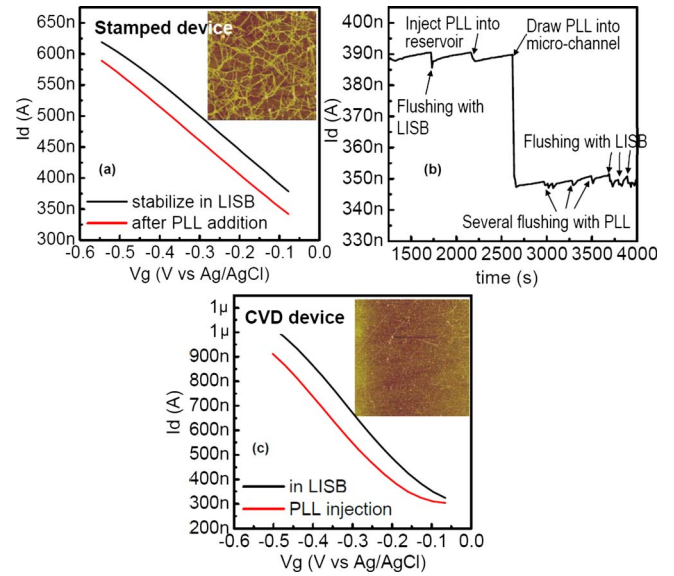


FIG. 2. (Color online) (a) Change in  $I_{sd}-V_g$  curve before (dark) and after (light) adsorption of 1 nM PLL in LISB solution. (b) Kinetic measurement of  $I_{sd}$  at  $V_g = -100$  mV vs Ag/AgCl [indicated by the dashed line in (a)] and  $V_d = 10$  mV, showing the change in conductance at respective biosensing steps. (c) Comparison of response signal between solution-prepared CNTFET and *in situ* grown CNTFET on Si substrate.

Further improvements in the stamped devices may be achieved by semiconducting tube enrichment<sup>10</sup> and possible alignment strategies<sup>11</sup> that have been recently reported in the literature.

The response sensitivity of the laminated LG-CNTFETs was investigated by a concentration-signal analysis of the sensor response toward PLL [Fig. 3(a), Table I]. Assuming that the diffusive transport, mobility ( $\mu$ ), and threshold voltage can be estimated using the transconductance in linear regime at  $V_d = 10$  mV,<sup>12</sup>

$$\mu = \frac{dI_d}{dV_g} \frac{1}{C_T} \frac{L}{W} \frac{1}{V_d},$$

where  $C_T \approx C_Q$  is the quantum capacitance per unit area of the network for liquid gate configuration.  $C_Q$  in the calculation was estimated from the quantum capacitance per unit length ( $C_{Ql}$ ) of individual SWCNT following the relationship:  $C_Q \sim (\partial N / \partial w) C_{Ql}$ , where  $N$  is the number of tubes and  $w$  is the width.<sup>13</sup> The linear density  $\partial N / \partial w$  is approximated to be in the range from 5 to 8  $\mu\text{m}^{-1}$  from AFM images. Taking the conservative value of 8  $\mu\text{m}^{-1}$ , together with  $C_{Ql} \sim 4 \times 10^{-10}$  F/m,  $C_Q$  is estimated to be  $\sim 3.2 \times 10^{-3}$  F/m<sup>2</sup>, yielding a mobility in the range of 27  $\text{cm}^2/\text{V s}$  (Table I), a value in agreement with other literature reports.<sup>13</sup> The calculated  $V_T$  shows a shift in negative direction and a saturated response above 10 pM of PLL.

Possible sensing mechanisms reported in the literature<sup>2,8,14,15</sup> include (i) electrostatic gating effect, (ii) Schottky barrier modulation, (iii) capacitance effect, and (iv) mobility change. In brief, electrostatic gating causes a threshold voltage shift; Schottky barrier modulation results in a decrease in  $I_{sd}$  at  $V_g < 0$  and increase in  $I_{sd}$  at  $V_g > 0$ ; capacitance effect, on the other hand, results in a decrease in gradient of the transfer characteristic at negative and positive  $V_g$ ; and mobility changes (possibly scattering induced) cause a decrease in  $I_{sd}$  at both positive and negative  $V_g$  regions. Upon PLL interaction with the LG-CNTFET, typified by Fig.

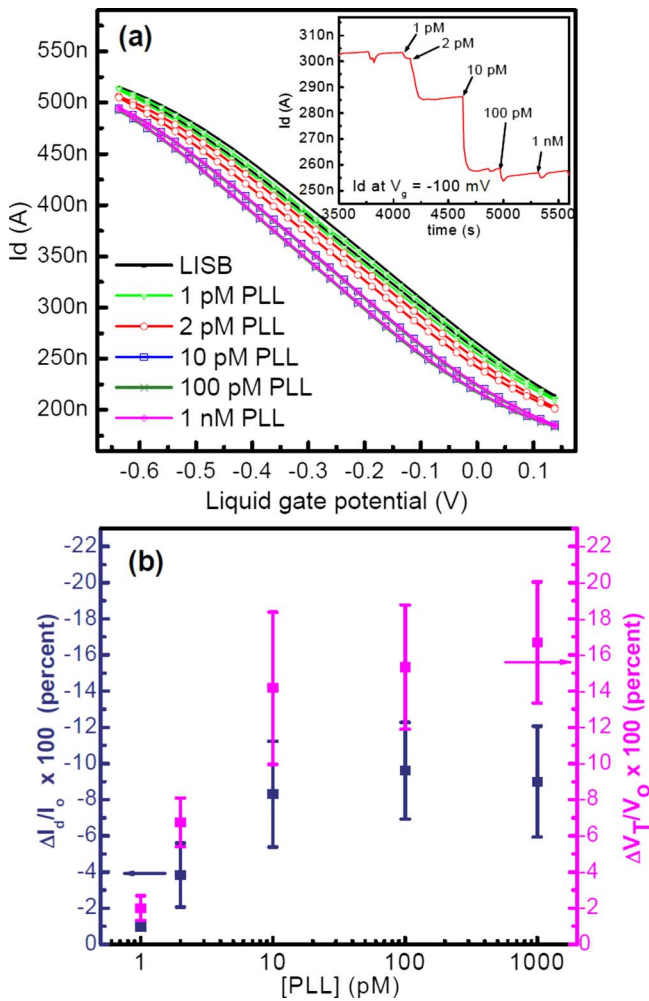


FIG. 3. (Color online) (a) Concentration dependence response of PLL in one device. Inset: kinetic measurement taken at  $V_g = -100$  mV and  $V_d = 10$  mV. (b) Changes in drain current and threshold voltage vs PLL concentration, normalized with respect to the  $I_{sd}$  and  $V_T$  signal of the bare device, collected from 20 different measurements.

3(a) and Table I, the  $I_{sd}-V_g$  curve showed a negative  $V_g$  shift ( $\Delta V_T < 0$ ), together with the relatively unchanged transconductance and mobilities at different PLL concentrations. The unchanged mobility rules out the Schottky barrier and other mechanisms, strongly suggesting that the active sensing mechanism in this study is related to the electrostatic gating effect, where the high positively charged PLL at  $pH \sim 7.5$  absorbs into the CNT network and induces a negative charge screening, thus shifting the  $I_{sd}-V_g$  curve toward negative gate voltages and leading to a reduction in  $I_{sd}$ .<sup>8</sup> The signal satu-

TABLE I. LG-CNTFET device response readings at different PLL concentrations.

Condition	Mobility (cm <sup>2</sup> /V s)	$V_T$ (V)	$\Delta V_T$ (V)	$I_d$ (nA) at $-100$ mV	$\Delta I_d$ (nA)
Bare device	27.10	0.61	0	314	0
1 pM	27.31	0.60	-0.01	310	-4
2 pM	27.56	0.56	-0.05	297	-16
10 pM	28.31	0.49	-0.12	269	-45
100 pM	28.31	0.48	-0.13	268	-46
1000 pM	28.31	0.49	-0.12	269	-45

ration beyond 10 pM concentrations may imply complete PLL coverage on the SWCNT network and possible steric hindrance effects that may prevent any additional absorption of PLL.

Figure 3(b) represents collection of data from more than 20 data points. The standard deviation of  $\Delta V_T$  and  $\Delta I_d$  measurements are in the range of 10%–15%. The device-to-device variability is attributed to various factors, including network density, bundle density, and ratio of metallic to semiconducting tubes among others. Limit of detection (LOD) in the laminated LG-CNTFET, approximately 1.01 pM, is determined from  $3\sigma_{\text{blank}}/S$ , where  $\sigma_{\text{blank}}$  is the standard deviation in blank solution and  $S$  is the sensitivity calculated from the slope of the sensor response<sup>16</sup> in the 0–10 pM range [Fig. 3(b)].

In summary, a practical approach of fabricating laminated LG-CNTFETs through a solution processed route involving only two materials, PDMS and SWCNT, is demonstrated. The laminated LG-CNTFETs show highly sensitivity response toward PLL with LOD, approximately 1 pM. As indicated by a negative threshold voltage shift, the sensing mechanism is primarily attributed to electrostatic interactions between the PLL and the SWCNTs. The methodology is readily extendable for applications using alternative polymers as the carrier medium as well as to other semiconductor materials including organic or inorganic semiconductors in thin film or nanowire forms.

The authors wish to thank Professor George Gruner, UCLA, for valuable discussions and inputs regarding this manuscript. Ju Nie Tey and I Putu Mahendra have contributed equally to this work.

- <sup>1</sup>S. N. Kim, J. F. Rusling, and F. Papadimitrakopoulos, *Adv. Mater. (Weinheim, Ger.)* **19**, 3214 (2007).
- <sup>2</sup>E.-L. Gui, L.-J. Li, P. S. Lee, A. Lohani, S. G. Mhaisalkar, Q. Cao, S. J. Kang, J. A. Rogers, N. C. Tansil, and Z. Gao, *Appl. Phys. Lett.* **89**, 232104 (2006).
- <sup>3</sup>K. Besteman, J.-O. Lee, F. G. M. Wiertz, H. A. Heering, and C. Dekker, *Nano Lett.* **3**, 727 (2003).
- <sup>4</sup>C. Li, M. Curreli, H. Lin, B. Lei, F. N. Ishikawa, R. Datar, R. J. Cote, M. E. Thompson, and C. Zhou, *J. Am. Chem. Soc.* **127**, 12484 (2005).
- <sup>5</sup>S. Rosenblatt, Y. Yaish, J. Park, J. Gore, V. Sazonova, and P. L. McEuen, *Nano Lett.* **2**, 869 (2002).
- <sup>6</sup>J. N. Barisci, G. G. Wallace, and R. H. Baughman, *J. Electroanal. Chem.* **488**, 92 (2000).
- <sup>7</sup>Y. Zhou, L. Hu, and G. Gruner, *Appl. Phys. Lett.* **88**, 123109 (2006).
- <sup>8</sup>I. Heller, A. M. Janssens, J. Mannik, E. D. Minot, S. G. Lemay, and C. Dekker, *Nano Lett.* **8**, 591 (2008).
- <sup>9</sup>E. D. Minot, A. M. Janssens, I. Heller, H. A. Heering, C. Dekker, and S. G. Lemay, *Appl. Phys. Lett.* **91**, 093507 (2007).
- <sup>10</sup>M. S. Arnold, A. A. Green, J. F. Hulvat, S. I. Stupp, and M. C. Hersam, *Nat. Nanotechnol.* **1**, 60 (2006).
- <sup>11</sup>M. C. LeMieux, M. Roberts, S. Barman, Y. W. Jin, J. M. Kim, and Z. Bao, *Science* **321**, 101 (2008).
- <sup>12</sup>E. Artukovic, M. Kaempgen, D. S. Hecht, S. Roth, and G. Gruner, *Nano Lett.* **5**, 757 (2005).
- <sup>13</sup>T. Ozel, A. Gaur, J. A. Rogers, and M. Shim, *Nano Lett.* **5**, 905 (2005).
- <sup>14</sup>Q. Fu and J. Liu, *J. Phys. Chem. B* **109**, 13406 (2005).
- <sup>15</sup>X. Tang, S. Bansarutip, N. Nakayama, E. Yenilmez, Y. Chang, and Q. Wang, *Nano Lett.* **6**, 1632 (2006).
- <sup>16</sup>L. Torsi, G. M. Farinola, F. Marinelli, M. C. Tanese, O. H. Omar, L. Valli, F. Babudri, F. Palmisano, P. G. Zamboni, and F. Naso, *Nature Mater.* **7**, 412 (2008).